Bulletin of Electrical Engineering and Informatics
Vol. 15, No. 3, June 2026, pp. 1911~1920
ISSN: 2302-9285, DOI: 10.11591/eei.v15i3.10297

Design and analysis of peaking capacitor for generation of high voltage fast risetime pulses

Madhu Palati[1], Manjunatha Babu Pattabhi[2], Ozwin Dominic Dsouza[2]
[1]Accenture Ltd., Bengaluru, India
[2]Department of Electrical and Electronics Engineering, BMS Institute of Technology and Management, Bengaluru, India

Article Info

Article history:

Received Mar 17, 2025
Revised Feb 5, 2026
Accepted Mar 10, 2026

Keywords:

Electric field
Marx generator
Peaking capacitor
Peaking switch
PSPICE software
Quick field

ABSTRACT

High voltage pulses of short duration are required in certain applications, here precise and rapid electrical energy delivery is required. These include applications like pulsed power system, high speed switching circuits, plasma generation circuits, high speed imaging, non-thermal food processing. One of the best and cheap methods of producing the high voltage fast rise time pulses is using Peaking capacitor. Designing a high-voltage peaking capacitor requires careful consideration of various factors such as voltage rating, capacitance value, energy storage capacity, physical size, dielectric material, and safety measures. In this paper, designing of 200 pF, 300 kV peaking capacitor is presented and simulation is carried out in PSPICE. The maximum peak voltage across the peaking capacitor, the time to reach peak voltage, and the maximum peaking current obtained are 290 kV, 98.9 ns, and 22.41 kA, respectively. Also, to study the electric field of the medium used in peaking capacitors, Quick field software is used. The maximum electric field in Perspex, used as a dielectric medium, was 13 kV/mm.

Corresponding Author:

Madhu Palati
Accenture Ltd.
Bengaluru, India
Email: mfmadhu@gmail.com

1. INTRODUCTION

In certain applications, electrical energy needs to be stored during low-demand periods and release it rapidly during peak demand. This can be achieved using Peaking capacitors, these are also known as pulse discharge capacitors and are specially designed to deliver the energy in short duration [1]. These finds in applications like pulsed lasers, particle accelerators, electromagnetic pulse (EMP) simulators [2], plasma generation for under water application [3], high-power microwave devices, radio detection and ranging (RADAR) systems, magnetic resonance imaging (MRI), pulse forming networks (PFN) for food processing, electromagnetic interference (EMI) testing, electromagnetic compatibility (EMC) measurements [4]-[6]. Care has to be taken while designing of peaking capacitor and choose the withstanding voltage to be greater than the peak voltage that appears across a peaking capacitor, else it may lead to flash over. Sometimes the design is based on the capacitance requirement. The capacitance value depends on factors such as the desired pulse duration, peak power, and energy requirements of the system. The design also, can be based on the dielectric material suitable for high-voltage applications. Common dielectric materials used in high-voltage capacitors include ceramic, film, and glass. The choice of dielectric material depends on factors such as operating temperature, voltage rating, and desired dielectric constant. Since these capacitors are involved in rapid discharge and charging cycles. Design safety measures such as appropriate insulation, discharge circuits, and protective enclosures to prevent electrical hazards. Safety considerations become crucial when dealing with

high voltages. Determine the physical size and configuration of the capacitor based on the available space and system requirements. Consider factors such as mounting options, cooling requirements, and mechanical stability. Based on the electrode design, which commonly include parallel plate, rolled foil, and stacked foil. Each electrode configuration has different performance and efficiency of the capacitor.

Depending on the application's specific needs, high voltage peaking capacitors can use a variety of dielectric materials. The choice of dielectric material depends on factors such as voltage rating, operating temperature, dielectric constant, dielectric loss, and physical properties. The most often utilized dielectric materials in high voltage peaking capacitors are ceramic, film, polypropylene (PP), polyethylene terephthalate (PET), Glass and Perspex. Ceramic offers strong dielectric strength, minimal dielectric loss, and great stability throughout a wide temperature range. Film capacitors utilize a thin film of dielectric material, typically made of materials such as polyester, polypropylene, PET, or polycarbonate [7]. Film capacitors are known for their high voltage ratings, low dielectric loss, and good stability over a wide frequency range. They are often employed in applications that need high energy density. Polypropylene capacitors, which are utilized in pulsed power systems, have outstanding electrical features such as high dielectric strength, low dielectric loss, and good self-healing [8]. Film capacitors provide good dielectric strength, low dielectric loss, and high breakdown voltage capabilities, used where stable and reliable operation is required. Glass capacitors utilize a glass dielectric material with high dielectric strength and low losses and used in high-energy physics experiments. Perspex of its excellent dielectric strength and transparent in nature is used in high voltage cylindrical capacitors. Apart from these air, sulphur hex fluoride (SF6), mixture of SF6 and air, Nitrogen.

Taherian *et al.* [9] presented two modular high-voltage pulse generator topologies derived from buck–boost converters operating in discontinuous mode. These topologies charge multiple capacitors simultaneously, enabling compact unipolar or bipolar bell-shaped pulses of up to 1 kV. Arbitrary pulse widths ranging from nanoseconds to microseconds can be achieved, and the design avoids the need for series-connected switches. However, a limitation of this topology is that the generated voltage is restricted to relatively low levels. High-voltage pulses are also used in electroporation-based cancer treatments. A multilevel converter with linear voltage regulation is employed in such applications. Since bus capacitance introduces challenges related to size and safety, the authors designed a system that significantly reduces the required bus capacitance while maintaining stable microsecond-range voltage output. Nevertheless, the output voltage pulses are still limited to a few kilovolts [10]. Ma *et al.* [11] have demonstrated an efficient, low-cost, multi-stage pulser that uses transmission lines for energy storage, variable-impedance boosting, and pulse stacking. This approach produces high-voltage, nanosecond-width pulses (10 kV, ≤12 ns) and is a promising design for applications requiring compact, high-performance pulse generators. Additionally, researchers in [12] investigated how high-frequency pulse-width modulation (PWM) stress affects partial discharge (PD) behavior in high-frequency transformers (HFT) insulation. It was observed that PD primarily occurs at triple junctions (conductor–insulation–air), where electric stress concentrates under square pulses. Repetitive PD activity leads to space charge accumulation, which modifies internal electric fields and influences subsequent PD behavior.

2. DESIGN OF PEAKING CAPACITOR

For generating standard impulse voltages Marx generator is commonly used. This generator produces waveshapes having a duration in a few microseconds to 100’s of microseconds. In the present work, a five stage Marx generator is considered and is shown in Figure 1, each stage comprises two 15 kV, 0.2 µF capacitors connected in series. Input source is single phase transformer of 35 kV fed from an autotransformer, and is rectified. Controlled DC can be fed to the Marx generator for charging the capacitors in parallel to the required DC voltage. The required gap spacing between the spherical gaps is determined so that breakdown does not occur during the charging process. After charging the capacitors to the proper voltage, the first spark gap is ignited using external triggering making the first stage and second stage capacitors get connected in series. The voltage of these two stages gets added up and appears across the next gap and resulting in the simultaneous breakdown of other gaps. The capacitors are discharged in series after being charged in parallel to the required voltage. The voltage of each capacitor gets added up and higher output voltage is produced at the output of the Marx generator [13]. This whole voltage (Vo) gets to appear across the test object (C_2) also, termed as load capacitance, in the present case the test load capacitance is considered as 2000 pF.

Marx’s equivalent capacitance is given by (1). The front time t_1 and tail time t_2 are given by (2) and (3) respectively. Due to dielectric losses in capacitors and losses in wave shaping resistors (R_1 and R_2), efficiency has to be considered while estimating the output voltage. The efficiency is given by (4). For generating a standard lightning impulse of duration 1.2 µs/50 µs, the values of wave shaping resistors R1 and

R2 obtained using (2) and (3) are 220 Ω and 3026 Ω respectively. The practical output voltage is given by (5). The energy rating (E) of the Marx is given by (6) [14].
Equivalent capacitance of Marx generator

$$C_1 = \frac{C}{n} = \left(\frac{(0.2\mu F/2)}{5}\right) = 0.02\ \mu F \quad (1)$$

$$t_1 = 3 * R_1 * \left(\frac{C_1 * C_2}{C_1 + C_2}\right) \quad (2)$$

$$t_2 = 0.7 * (R_1 + R_2) * (C_1 + C_2) \quad (3)$$

$$\eta_{Marx} = \left(\frac{R_2}{R_1 + R_2}\right) * \left(\frac{C_1}{C_1 + C_2}\right) \quad (4)$$

$$\text{Marx Output voltage } V_p = \eta * \text{no of stages (n)} * \text{stage charging Voltage } (V_C) \quad (5)$$

$$E = \frac{1}{2} * C_1 V_o^2 \quad (6)$$

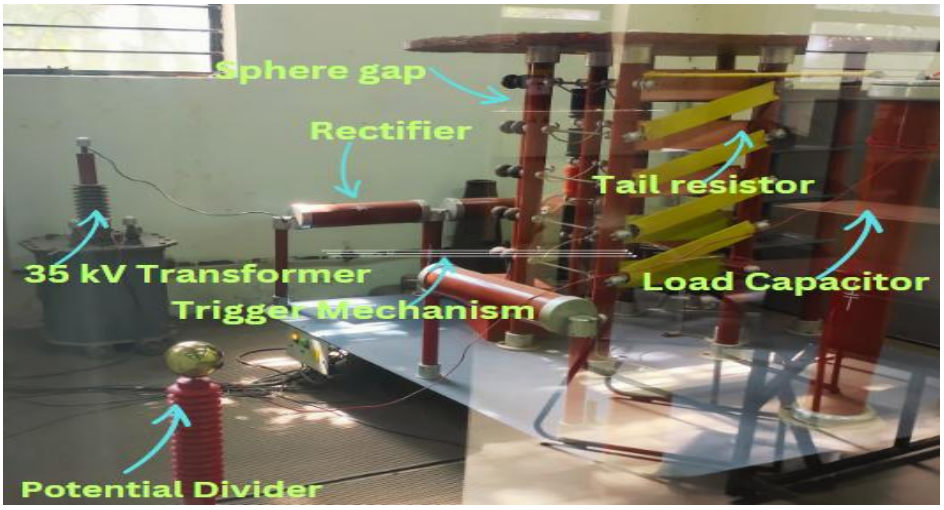

Figure 1. Experimental setup of a five stage 150 kV, 225J Marx generator

By considering 30 kV as the full rated voltage of each stage, the ideal output voltage of this five stage Marx generator is 150 kV. The estimated efficiency of Marx using (4) is 84.74%. Therefore, the peak output voltage considering the efficiency will be less than the ideal output voltage. The estimated peak output voltage of Marx using (5) is 127.12 kV. The energy rating of the Marx is estimated using (6) and is equal to 225 J. Figure 2 displays the lightning impulse output waveform of the Marx generator, with rise and tail times of 1.3 µs and 45 µs, respectively. The errors in the theoretical and experimental values are 8.3% and 10% respectively with respect to front time and tail time of a lightning impulse and these are well within the limits of standard lightning impulse waveform (30% and 20%).

For generating wave shapes with short duration in the order of nanoseconds or picoseconds it is difficult to produce these waveforms with Marx generator alone, this is due to the internal inductance of the Marx generator which practically limits the application to generate high voltage impulses of short duration [15]. In addition to Marx generator, peaking capacitor can be used to generate the impulse waveforms of duration nano seconds to sub nano seconds [16]. Figure 3 shows the block diagram for the Marx generator and peaking capacitor circuit. A peaking circuit is made up of a load, a peaking switch, and a peaking capacitor. Peaking capacitor and peaking switch are of low inductance in the order of nano Henrys [17]. Marx generator delivers output power to Peaking capacitor and it gets charged to almost double the Marx output voltage (Vp) and during this period peaking switch is in an open condition. Due to the low inductance of peaking circuit, generally in the order of few nano Henrys to tens of nano Henrys (this inductance is very much less than Marx circuit), the peaking capacitor discharges the power into the load through a peaking switch at a fast rate [18]-[20]. Nowadays, for fast switching operations without any jitter, conventional spark

gaps are replaced with IGBTs [21]-[23]. The peaking capacitor has to be designed with low inductance and generally cylindrical capacitor configuration is preferred in high voltage pulsed field applications. The peaking capacitor will have a far smaller value than Marx's equivalent capacitance. In the present work, peaking capacitor is considered of 200 pF and designed to withstand 300 kV. Commercially hollow cylinders of different sizes starting from 6 mm to 500 mm are easily available in the market. Inner electrode of 50 mm and one meter length is considered, and the outer diameter is estimated based on the dielectric medium. In (7) describes the capacitance of a cylindrical capacitor and the value of outer diameter for different dielectric medium is estimated and shown in Table 1.

$$C_P = \frac{2\pi\,\varepsilon_o\,\varepsilon_r\,l}{ln\left(\frac{D}{d}\right)} \tag{7}$$

where, absolute permittivity of free space (ε_o)=8.854×10^{-12} F/m, relative permittivity (ε_r) depends on the type of the dielectric medium, l is the length, D is the diameter of the outer electrode, and d is the diameter of the inner electrode.

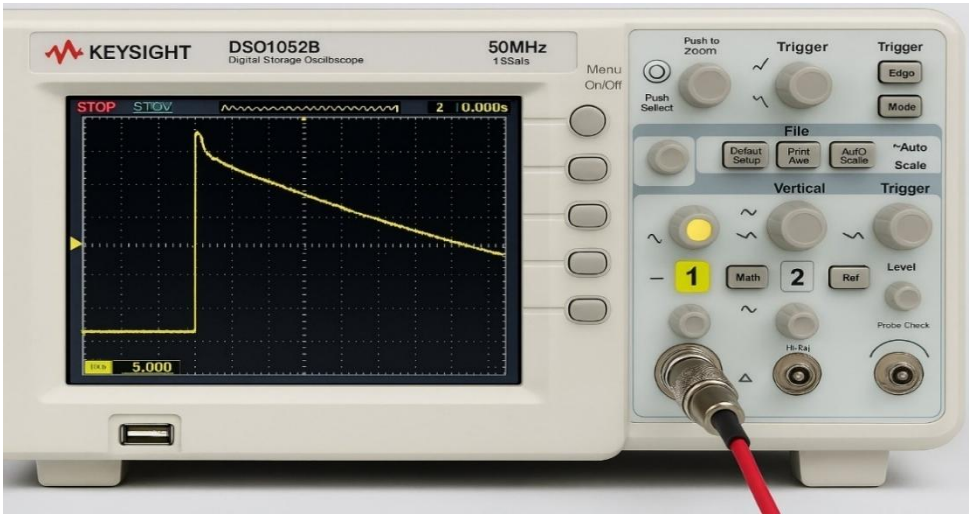

Figure 2. Impulse voltage output waveform of Marx generator

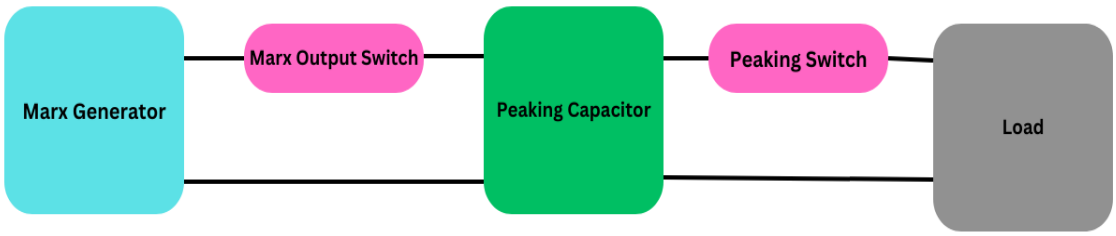

Figure 3. Block diagram of Marx generator and peaking circuit

Table 1. Parameters of cylindrical capacitor

S. No	Dielectric medium	Relative permittivity	Inner electrode (mm)	Outer electrode (mm)
1	Air	1	50	66
2	Polypropylene	2.2	50	92
3	SF_6	1.3	50	72
4	Perspex	3.3	50	125

In (8) describes the internal inductance of the peaking capacitor.

$$L_P = \frac{\mu_o}{2\pi} * ln\left(\frac{D}{d}\right) * length\ in\ meters \tag{8}$$

μ_o is absolute permeability of free space=$2\,\pi\,x\,10^{-7}\,H/m$.

3. ELECTRIC FIELD ANALYSIS OF PEAKING CIRCUIT

To study the breakdown strength of the dielectric medium, simulation must be performed to save time and cost before going for fabrication [24], [25]. In this work Simulation is carried on high voltage cylindrical capacitor shown in Figure 4. Proper design of the capacitor can be done by analyzing the simulation results with theoretical values. An electric field in a cylindrical capacitor is estimated using (9). Simulation is carried out in Quick field program for the model presented in Figure 4(a) representing the structure of cylindrical capacitors and Figure 4(b) represents the estimation of the electric field in the dielectric medium, and the simulation output is displayed.

$$E = \frac{2V_p}{d*ln\left(\frac{D}{d}\right)}\ v/m \tag{9}$$

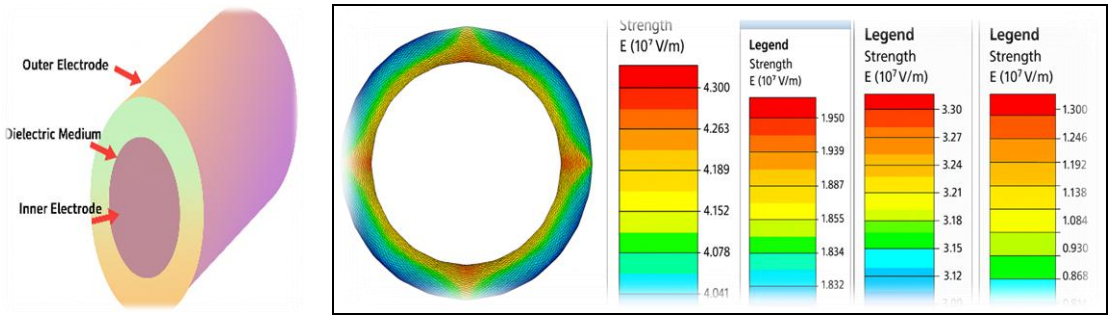

(a) (b)

Figure 4. High voltage cylindrical capacitor; (a) sketch of cylindrical capacitor and (b) simulation of electric field analysis with different dielectric medium

Perspex (also known as acrylic or polymethyl methacrylate, PMMA) is often preferred as a dielectric material in peaking capacitor design over alternatives like air, polypropylene, or SF_6 due to a combination of electrical, mechanical, and practical advantages as shown in Table 2.

Table 2. Comparison of Perspex as dielectric with other popular materials

Property	Perspex	Air	Polypropylene	SF_6 gas
Dielectric strength	High (~13 kV/mm)	Low (~3 kV/mm)	Very high (~20–30 kV/mm)	Very high (~89 kV/cm)
Mechanical stability	Excellent	Poor	Good	Poor (gas)
Fabrication ease	Easy	N/A	Moderate	Complex
Environmental impact	Low	Low	Low	High (GHG)
Cost	Moderate	Low	Low	High

From (7), it is evident that the higher the dielectric constant, the higher the capacitance, and the more energy can be stored. When a dielectric with relative permittivity ε_r is introduced, the electric field inside the dielectric decreases compared to vacuum or air, and the field is redistributed based on the dielectric constant—especially in multi-layer dielectrics. A high ε_r material like Perspex reduces field stress, improves insulation, and may exhibit dielectric relaxation or losses, which can affect the pulse rise time depending on the extent of dielectric loss. Higher ε_r leads to high capacitance and longer discharge time and pulse width will be more and vice versa. In high-voltage pulse circuits, inductance affects the rise time and shape of the discharge pulse. Higher the inductance slower discharge (longer pulse duration). In pulsed power systems, both are tuned to achieve desired pulse width and energy delivery.

4. SIMULATION OF PEAKING CIRCUIT

To investigate the output waveform of the high voltage Marx generator as shown in Figure 5, an equivalent circuit was created, and simulation was performed in PSPICE. The equivalent circuit of 150 kV, 225 J Marx generator is shown in Figure 5(a) and the simulation output of Marx lightning impulse peak voltage (kV) versus time (ns) is shown in Figure 5(b). Figure 6 shows the Marx with Peaking capacitor, Figure 6(a) depicts the Marx circuit, including the peaking circuit, and Figure 6(b) shows the voltage across the peaking capacitor (kV) versus the time (ns) prior to shutting the switch. The output load current and prepulse current are shown in Figure 7. The output current (kA) in the load versus time (ns) is shown in

Figure 7(a) and prepulse current (amps) versus the time (ns) is shown in Figure 7(b) respectively. In (10) shows the load circuits characteristic impedance and is given by:

$$Z_{Out} = \sqrt{\frac{(L_p+L_{ps})}{C_p}} = \sqrt{\frac{10\ nH}{200pF}} \approx 7\ ohms \quad (10)$$

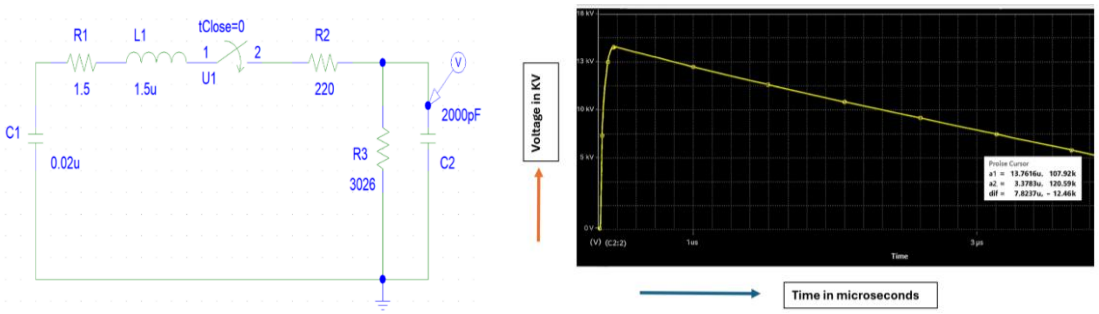

Figure 5. High voltage Marx generator; (a) equivalent circuit of 150 kV, 225 J Marx generator and (b) simulation waveform of voltage across load capacitance (kV) versus time (µs)

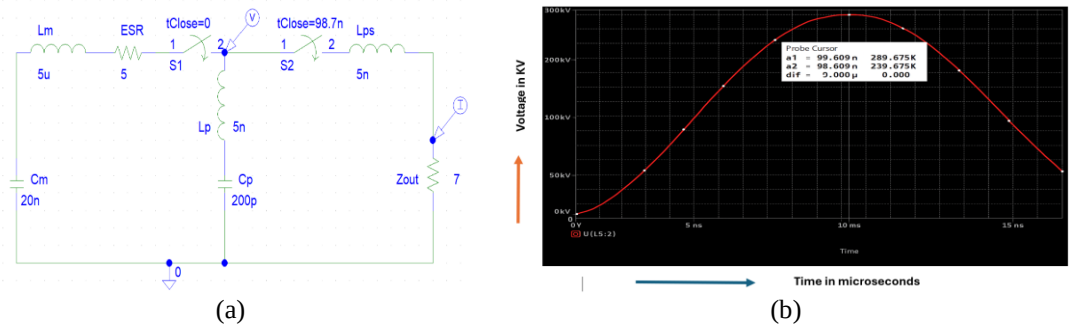

Figure 6. Marx generator with peaking capacitor; (a) equivalent circuit of Marx circuit with peaking circuit and (b) simulation waveform of Peak voltage (kV) across the peaking capacitor versus time (ns)

To study the effect of spark gap capacitance, on pre-pulse current, a capacitance of 0.1 nF to 1 nF is connected across the peaking switch to study the effect of pre-pulse current. A current of 1645 A flow in the circuit before closing the peaking switch and a voltage of 11.52 kV exists across the load. A current of 633 A flow in the circuit before closing the peaking switch and a voltage of 4.43 kV exists across the load. For Csg=0.1 nF, 360 A flow in the load circuit as shown in Figure 7(a), and 2.52 kV exists across the load. The prepulse current is shown in the Figure 7(b). More the spark gap capacitance, larger will be the pre-pulse current. Furthermore, the time required for the voltage wave to reach its peak value increases by one to two nanoseconds. The magnitude of the voltage waveform will be reduced by one to two kilovolts. The variation in magnitude of peak voltage and peak time is minimal.

By using sharply pointed conical electrodes as a peaking switch, the electric field becomes concentrated, leading to early ionization. Surface polishing prevents premature breakdown, and adjusting the pressure helps tune the breakdown voltage and suppress pre-pulse conduction. Precise control can be achieved by using a trigger electrode or a trigatron gap electrode arrangement. In high-voltage Marx generators, several limitations affect performance, safety, and long-term reliability. Breakdown voltage limitations can be due to poor insulation, unequal voltage sharing across each stage and environmental factors. Parasitic inductance causes pulse distortion, energy loss and switching stress. Long term reliability has an impact on aging, partial discharge and thermal cycling. Automated diagnostics in Marx generators with peaking circuits can improve reliability through real-time monitoring, enhance understanding of pulse behavior under varying load and environmental conditions. Other methods of high-voltage pulse generation include the Blumlein line, which produces rectangular pulses but is limited by its line length. Transmission line transformers (TLTs) have limited energy capacity and involve complex design and fabrication. Therefore, these two methods are not considered in this work for generating high-voltage fast pulses.

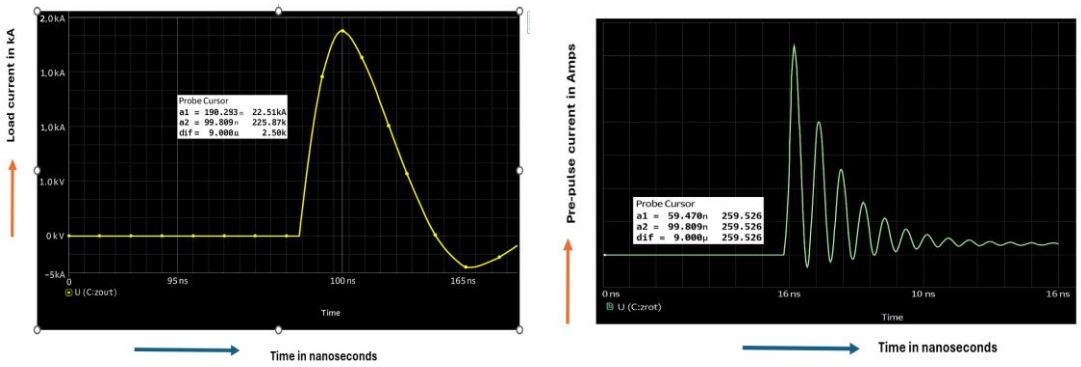

(a) (b)

Figure 7. Output load current and prepulse current; (a) simulation waveform of load current (kA) versus time in nanoseconds and (b) simulation waveform of prepulse current (kA) in peaking circuit versus time in nanoseconds

5. RESULTS AND DISCUSSION

The dielectric used in the cylindrical capacitor plays an important role in deciding the parameters of the peaking capacitor and from the estimation of the breakdown strength of the dielectric medium, it becomes easy for proper choice of dielectric material and the main parameters are shown in Table 1. It is found that for fixed inner electrode diameter and peaking capacitor values, as the relative permittivity increases, the outer diameter increases. The electric field for different dielectric medium is tabulated in Table 3 and it is observed that if we use air as medium for the designed configuration the electric field is high on the surface of inner electrode and there is chance flashover takes as the breakdown strength in pulsed fields for air is around 10 to 15 kV/mm and in the present case it is 43 kV/mm. In the remaining cases of Polypropylene, SF6 and Perspex, the values are well within the limits [26], [27]. Perspex is preferred in this case as the electric field is 13 kV/mm and the breakdown strength of Perspex when subjected to impulse wave is 20 kV/mm to 25 kV/mm [28]. The electric field theoretical values and simulation values obtained for different dielectric medium are matching.

Table 3. Electric field in peaking capacitor for different dilectric materials

S.No	Dielectric medium	Relative permittivity	Electric field theoretical (kV/mm)	Electric field simulation (kV/mm)
1	Air	1	43.16	43
2	Polypropylene	2.2	19.62	19.6
3	SF_6	1.3	33.2	33
4	Perspex	3.3	13.08	13

From Figure 6(a), performing the analysis for primary loop i.e., Marx circuit and the peaking capacitor and after comparing the obtained equation with a standard second order equation, the maximum output voltage across the peaking capacitor is given by (11) and time to reach peak voltage [29] is given by (12):

$$V_P(t) = 1.486\, x\, 10^5 * \left[1 + e^{\left(\frac{-\sigma\pi}{\sqrt{1-\sigma^2}}\right)}\right] \quad (11)$$

$$t_p = \frac{\pi}{\omega\sqrt{1-\sigma^2}} \quad (12)$$

Where the angular frequency (ω) and damping ratio (σ) are $31.749 * 10^6$ rad/ sec and $15.732 * 10^{-3}$ respectively. To determine the current in the load circuit, the secondary loop is considered for analysis which include peaking capacitor, peaking switch and load. After comparing with the standard form [25] the current in the load circuit is given by (13):

$$I(t) = 47.199 *\ 10^3 *\ e^{-(0.35*10^9 t)} * sin(0.614 * 10^9 t) \quad (13)$$

From PSPICE simulation as shown in Figure 7(a), the time to reach peak value of current from 98.7 ns to 100.283 ns is 1.583 ns. This time has to be submitted in (13) to obtain peak current in the load

circuit. Practically, the breakdown voltage for the same gap distance and time taken may vary based on the type of peaking switch configuration, the inductance of the peaking capacitor, peaking switch and the load inductance [30]. The simulation results obtained from PSPICE and theoretical results are tabulated in Table 4. From Table 4, it is observed that the theoretical values and simulation values are matching and hence the results obtained are validated. Marx with peaking circuit the ideal peak voltage to be 300 kV from simulation it is 289.67 hence the efficiency is 96.5%.

Table 4. Simulation and theoretical results of Peaking circuit

S. No	Parameters	Theoretical	Simulation	% error
1	Peaking capacitor voltage	290 kV	289.675 kV	0.12
2	Time to reach peak voltage	98.963 ns	98.7 ns	0.26
3	Peak load current	22.41 kA	22.51 kA	0.44

Some of the practical challenges in measuring the fast rise time (tens of nano seconds) high voltage impulse voltage is requirement of high-bandwidth and high-sampling-rate oscilloscopes, measurement probes and cables introduce parasitic inductance and capacitance, which can distort fast transients, cause EMI, measurement errors due to non-linearities or bandwidth limitations and availability of standard stainless steel hollow cylinder dimensions in market. The above stated problems can be minimised with high-voltage capacitive divider, digital storage oscilloscope with ≥1 GHz bandwidth, fiber-optic isolated probes for EMI immunity and pulse generator with controlled rise time for calibration.

Faster discharge (nanosecond pulses) requires low inductance and minimal parasitic elements (difficult to design) but often results in lower energy efficiency due to higher switching losses and EMI. Slower pulses allow better energy transfer and reduce stress on components but may not be suitable for applications like plasma generation or medical ablation that require sharp, high-energy pulses. Dielectric materials with high permittivity (ε_r) increase capacitance, enabling more energy storage, but may suffer from lower breakdown strength or higher dielectric losses. Electrode and encapsulation materials affect thermal stability, partial discharge resistance, and long-term reliability. In real time it is observed that capacitance and insulation properties vary with temperature, impacting pulse shape and reliability. Repetitive high-voltage pulses can cause insulation breakdown, partial discharge, and space charge accumulation. Real-world circuits include stray inductance and capacitance that distort ideal pulse shapes and reduce efficiency. Hence, utmost care must be taken during design stage itself considering voltage overshoot, LC resonance, EMI shielding, and grounding.

6. CONCLUSION

In this work, an attempt was made to design a 200 pF peaking capacitor for generating nanosecond pulses and this capacitor was used in conjunction with existing 150 kV, 225 J Marx generator to obtain double the Marx output voltage. The theoretical and PSPICE simulation results obtained are in close agreement which validates the results. It is preferred to use Perspex as the dielectric medium in peaking capacitor for safe operation and the electric field obtained from Quick field software and theoretical estimated values are closely matched. There is pre-pulse current in the peaking circuit before peaking switch closes, to reduce the pre-pulse current and the effect of spark gap capacitance. Few methods like triggerred spark gap, solid state switches, SF6 Spark gap exist in commercial market but due to limitations of each method, it is preferred to go for needle- needle configuration. This configuration reduces the spark gap capacitance. From analysis and simulation possibility of achieving high voltage nano second pulses is presented. Practical measurement of the high-voltage pulse across the peaking capacitor requires a Rogowski coil and a high-bandwidth oscilloscope. In the present work, due to the unavailability of these instruments, the fast rise-time high-voltage pulse was not measured.

FUNDING INFORMATION

Authors state there is no funding involved.

AUTHOR CONTRIBUTIONS STATEMENT

This journal uses Contributor Roles Taxonomy (CRediT) to recognize individual author contributions, reduce authorship disputes, and facilitate collaboration.

Name of Author	C	M	So	Va	Fo	I	R	D	O	E	Vi	Su	P	Fu
Madhu Palati	✓					✓				✓	✓	✓		
Manjunatha Babu Pattabhi		✓		✓		✓		✓	✓	✓	✓		✓	
Ozwin Dominic Dsouza		✓	✓	✓	✓		✓		✓					

C : **C**onceptualization
M : **M**ethodology
So : **So**ftware
Va : **Va**lidation
Fo : **Fo**rmal analysis
I : **I**nvestigation
R : **R**esources
D : **D**ata Curation
O : Writing - **O**riginal Draft
E : Writing - Review & **E**diting
Vi : **Vi**sualization
Su : **Su**pervision
P : **P**roject administration
Fu : **Fu**nding acquisition

CONFLICT OF INTEREST STATEMENT

Authors state no conflict of interest.

DATA AVAILABILITY

The authors confirm that the data supporting the findings of this study are available within the article.

REFERENCES

[1] W. Jia *et al.*, "A 800 kV compact peaking capacitor for nanosecond generator," *Review of Scientific Instruments*, vol. 85, no. 9, Sep. 2014, doi: 10.1063/1.4895158.

[2] H. Schilling, J. Schlueter, M. Peters, K. Nielsen, J. T. Naff, and H. G. Hammon, "High voltage generator with fast risetime for EMP simulation," in *Digest of Technical Papers-IEEE International Pulsed Power Conference*, 1995, vol. 2, pp. 1359–1364, doi: 10.1109/ppc.1995.599806.

[3] Z. Li *et al.*, "Effects of Output Peaking Capacitor on Underwater-Streamer Propagation," *IEEE Transactions on Plasma Science*, vol. 37, no. 10, pp. 1987–1992, Oct. 2009, doi: 10.1109/TPS.2009.2025376.

[4] R. Sundararajan, G. R. Nagabhushana, N. K. Kishore, and E. Soundarajan, "Influence of peaking capacitors in reducing rise times of high-voltage nanosecond pulses," *IEEE Transactions on Industry Applications*, vol. 41, no. 3, pp. 690–697, May 2005, doi: 10.1109/TIA.2005.847292.

[5] S. Bindu, M. Parekh, H. A. Mangalvedekar, A. Sharma, and D. P. Chakravarthy, "Modelling and analysis of high pressure peaking switch," in *23rd International Conference on High Pressure Science and Technology (AIRAPT-23)*, vol. 377, no. 1, p. 012098, Jul. 2012, doi: 10.1088/1742-6596/377/1/012098.

[6] T. A. Holt, M. B. Lara, C. Nunnally, and J. R. Mayes, "Compact Marx generators modified for fast risetime," in *PPC2009 - 17th IEEE International Pulsed Power Conference*, Jun. 2009, pp. 1197–1200, doi: 10.1109/PPC.2009.5386432.

[7] O. G. Gnonhoue, A. Velazquez-Salazar, É. David, and I. Preda, "Review of technologies and materials used in high-voltage film capacitors," *Polymers*, vol. 13, no. 5, pp. 1–19, Feb. 2021, doi: 10.3390/polym13050766.

[8] Z. Y. Ran, B. X. Du, M. Xiao, H. L. Liu, and J. W. Xing, "Dielectric Property Improvement of Polypropylene Films Doped with POSS for HVDC Polymer Film Capacitors," *IEEE Transactions on Dielectrics and Electrical Insulation*, vol. 28, no. 4, pp. 1308–1316, Aug. 2021, doi: 10.1109/TDEI.2021.009694.

[9] M. Taherian, S. Roshan, M. Allahbakhshi, E. Farjah, and T. Ghanbari, "A Modular Unipolar/Bipolar High-Voltage Pulse Generator Suitable for High Resistive Load," *IEEE Transactions on Plasma Science*, vol. 51, no. 5, pp. 1279–1289, May 2023, doi: 10.1109/TPS.2023.3262153.

[10] H. Sarnago, J. M. Burdio, and O. Lucia, "Electroporation Pulse Generator for Biomedical Applications with Improved Output Voltage Ripple and Reduced Bus Capacitor," *IEEE Transactions on Power Electronics*, vol. 38, no. 6, pp. 6774–6778, Jun. 2023, doi: 10.1109/TPEL.2023.3240244.

[11] J. Ma *et al.*, "10 kV nanosecond pulse generator with high voltage gain and reduced switches," *High Voltage*, vol. 9, no. 5, pp. 1059–1067, Oct. 2024, doi: 10.1049/hve2.12470.

[12] Z. Wang *et al.*, "Partial Discharge Behavior of High-Frequency Transformer Insulation Under High-Voltage PWM Stress," *IEEE Transactions on Power Electronics*, vol. 40, no. 9, pp. 13142–13156, Sep. 2025, doi: 10.1109/TPEL.2025.3566999.

[13] E. Kuffel, W. S. Zaengl, and J. Kuffel, *High Voltage Engineering Fundamentals*, 2nd ed. Newnes, pp. 61-65, 2000.

[14] M. Abdel-Salam, H. Anis, A. El-Morshedy, and R. Radwan, *Theory and Practice, 2nd ed., Revised and Expanded*, CRC Press, Boca Raton, Fla, USA, pp.541-546, 2000.

[15] B. Cadilhon, L. Pécastaing, T. Reess, and A. Gibert, "Low-stray inductance structure to improve the rise-time of a Marx generator," *IET Electric Power Applications*, vol. 2, no. 4, pp. 248–255, Jul. 2008, doi: 10.1049/iet-epa:20070250.

[16] J. Ma, L. Yu, L. Ren, Y. Liao, S. Dong, and C. Yao, "High Voltage Nanosecond Pulse Generator based on Inductive Energy Storage With Adjustable Pulse Width," in *2022 IEEE International Conference on High Voltage Engineering and Applications (ICHVE)*, Sep. 2022, pp. 1–4, doi: 10.1109/ICHVE53725.2022.9961737.

[17] J. Li, Y. Wang, S. He, X. Chen, and A. Qiu, "Compact pulse generator with sub-nanosecond rise time based on inductance of order of several nH," *Review of Scientific Instruments*, vol. 93, no. 8, Aug. 2022, doi: 10.1063/5.0101573.

[18] J. Mao *et al.*, "A compact, low jitter, nanosecond rise time, high voltage pulse generator with variable amplitude," *Review of Scientific Instruments*, vol. 83, no. 7, Jul. 2012, doi: 10.1063/1.4737146.

[19] B. J. Baliga, "IGBT Applications: Other," in *The IGBT Device*, 2nd ed., Elsevier, 2023, pp. 647–706, doi: 10.1016/b978-0-323-99912-0.00025-8.

[20] H. Devarajan, G. S. Punekar, and N. K. Kishore, "Design of an HV capacitor using the inherent advantage of charge simulation method and experimentations," *IET Science, Measurement and Technology*, vol. 12, no. 1, pp. 126–131, Jan. 2018, doi: 10.1049/iet-smt.2017.0121.
[21] P. Deb, B. Sethi, L. Rongali, M. Meena, R. Verma, and A. Sharma, "Generation of high voltage nanosecond pulses using Pulse Sharpening switch," in *2021 1st International Conference on Power Electronics and Energy (ICPEE)*, Jan. 2021, pp. 1–5, doi: 10.1109/ICPEE50452.2021.9358472.
[22] N. S. Pinjari and S. Bindu, "Analysis of a Solid-State Switch as Peaking Switch in a Solid-State Marx Generator," in *2022 Second International Conference on Next Generation Intelligent Systems (ICNGIS)*, Jul. 2022, pp. 1–6, doi: 10.1109/ICNGIS54955.2022.10079746.
[23] S. Bindu, S. B. Umbarkar, H. A. Mangalvedekar, A. Sharma, P. C. Saroj, and K. C. Mittal, "Peaking capacitor parameter evaluation with transfer function model," *IEEE Transactions on Plasma Science*, vol. 42, no. 2, pp. 336–339, Feb. 2014, doi: 10.1109/TPS.2013.2294344.
[24] M. Xiao, M. Zhang, H. Liu, B. Du, and Y. Qin, "Dielectric Property and Breakdown Strength Performance of Long-Chain Branched Polypropylene for Metallized Film Capacitors," *Materials*, vol. 15, no. 9, pp. 1–16, 2022, doi: 10.3390/ma15093071.
[25] A. Deshpande, G. V. Prakash, U. Goswami, R. Singh, and V. P. Anitha, "Implementation of Line Type High Voltage Nanosecond Rectangular Pulse Generator with Adjustable Pulse Widths for Liquid Discharge Applications," in *2019 IEEE Pulsed Power & Plasma Science (PPPS)*, Jun. 2019, pp. 1–5, doi: 10.1109/PPPS34859.2019.9009998.
[26] E. Onal, "Breakdown mechanism of different sulphur hexafluoride gas mixtures," *Advances in Materials Science and Engineering*, pp. 1–4, Jan. 2018, doi: 10.1155/2018/3206132.
[27] D. B. Watson, "Dielectric Breakdown in Perspex," *IEEE Transactions on Electrical Insulation*, vol. EI-8, no. 3, pp. 73–75, Sep. 1973, doi: 10.1109/TEI.1973.299247.
[28] A. Küchler, *High Voltage Engineering*. Berlin, Germany: Springer, 2018.
[29] B. S. Manke, *Linear control systems*, 5th ed. New Delhi, India: Khanna Publishers, 2010.
[30] M. Balmelli *et al.*, "Experimental analysis of breakdown with nanosecond pulses for spark-ignition engines," *IEEE Access*, vol. 9, pp. 100050–100062, 2021, doi: 10.1109/ACCESS.2021.3095664.

BIOGRAPHIES OF AUTHORS

Madhu Palati received the B.Tech. degree in Electrical and Electronics Engineering from Sri Venkateshwara University, Tirupati, in 2003, M.E. from M.S. University, Baroda, in 2005 and Ph.D. from Jain University, Bangalore in June 2016. He has worked as a software Engineer in Keane India Ltd, Gurgaon for a period of one and half years and in IBM Private Limited, Bangalore for a period of three years. He has worked as Assistant Professor in the Department of Electrical and Electronics Engineering, School of Engineering and Technology, Jain University, Bangalore for a period of seven and half years and worked as Assistant Professor in BMS Institute of Technology and Management, Bangalore for a period of 8 years. He is currently working as power system engineer at Accenture, Bangalore. He can be contacted at email: mfmadhu@gmail.com.

Manjunatha Babu Pattabhi received B.E. degree in Electrical and Electronics Engineering from Golden Valley Institute of Technology, K G F in 2004. M.E. Degree in Power and Energy System from University Visveshwaraiah College of Engineering in 2010. Ph.D. degree in Electrical Science from Visveshwaraiah Technological University in 2023. He is currently working as Assistant Professor in BMS Institute of Technology and Management, Bengaluru in the Department of Electrical Engineering. His research interests include power and energy system and FACTs controllers. He can be contacted at email: manjubabup@bmsit.in.

Ozwin Dominic Dsouza received B.E. degree in Electrical and Electronics Engineering and M.E. in Computer Applications in Industrial Drives from Visveshwaraiah Technological University (VTU) in 2005 and 2010 respectively. He is currently working as Assistant Professor in BMS Institute of Technology and Management, Bengaluru in the Department of Electrical Engineering since 2012. He is pursuing his Ph.D. in VTU and his research interests include power electronics, electric drives, power factor correction (PFC), and high voltage engineering. He can be contacted at email: ozwindsouza@bmsit.in.